

Generating Realistic Two-Line Elements for Notional Space Vehicles and Constellations

Troy Rockwood, Greg Steeger, Matthew Stein

March 9, 2022

Abstract

As space becomes increasingly populated with new satellites and systems, modeling and simulating existing and future systems becomes more important. The two-line element set has been a standard format for sharing data about a satellite’s orbit since the 1960s, and well-developed algorithms can predict the future location of satellites based on this data. In order to simulate potential future systems, especially when mixed with existing systems, data must be generated to represent the desired orbits. We present a means to create two-line element sets with parameters that closely resemble real satellite behavior, and rely on a novel approach to calculate the mean motion for even greater accuracy.

1 Introduction

The population of active satellites in orbit around Earth has increased exponentially over the last few decades[1]. Commercial, civil, and government entities continue to expand their role and influence in space. Modeling and simulation of satellites and their behavior has likewise increased. The use cases include constellation planning, optimization, performance assessment, and conjunction analysis[2, 3, 4].

There are many software tools and algorithms to simulate satellites and constellations of satellites. Among these is the well-known simplified perturbations model, often referred to as SGP4[5]. These algorithms make use of two-line element sets (TLEs)[6, 7] to describe the orbit of each satellite and begin the simulation. Regardless of the algorithm employed, TLEs are widely used and published for most active and inactive objects in orbit.

For the purposes of planning future space systems, it is useful to simulate satellites and orbits that do not yet exist, possibly alongside real systems already

in orbit. Doing so requires the generation of TLEs for the notional systems. A naïve approach based only on classical orbital elements might look like the following:

1. The desired inclination, eccentricity, altitude at perigee, and argument of perigee are chosen according to the desired orbit
2. The first and second derivative of mean motion and drag terms are set to exactly zero
3. The mean motion is calculated from Kepler’s third law using the altitude at perigee and a mean radius of the Earth of 6,371 km
4. The rest of the TLE elements are freely chosen, and the checksum is computed for the last character in each line

The classical orbital elements in Step 1 are freely chosen, but Step 2 and 3 each present opportunities for significant error in the desired simulation results. When propagating TLEs, some or all of the terms in

Step 2 help model realistic orbital decays depending on the algorithm chosen. Simulated notional TLEs may thus behave quite differently than TLEs created for orbiting satellites, making mixed simulations less realistic especially as simulation time increases. Similarly, calculating mean motion from a fixed value for the radius of the Earth presents potential for significant error in drift. Because the Earth is not a perfect sphere, gravitational effects experienced by satellites will be a function of the intended orbit, namely the inclination, eccentricity, and argument of perigee.

In order to realistically simulate the behavior of satellites, the generated TLEs should contain terms that accurately resemble those of real systems. We describe a novel method for generating TLEs for almost any notional system including realistic terms for drag and the first and second derivative of mean motion. Additionally, we describe a novel way to determine the mean motion (MM) for the desired orbit which is a function of inclination, eccentricity, and the argument of perigee. Finally, we summarize our approach which is an expansion of the above steps in Section 6, including a polynomial approach to determining the mean radius of the Earth for computing the mean motion.

2 Essential TLE Terms

This study ignores the title line sometimes included in some TLEs, and focuses only on lines one and two. A detailed visualization and explanation of each TLE term is illustrated in Figure 1 of Ref [6]. The satellite catalog number, classification, international designator value, element set number, and revolution number can all be chosen at will, and do not affect the simulation. The only exception is that satellite catalog numbers should not conflict with other satellites in the simulation. Additionally, the ephemeris type should be 0.

The epoch of the TLE can be chosen at will, but in generating an epoch one should consider the following implications. If a simulation only involves notional systems, then it is only important that all TLEs in the simulation have a similar epoch. If mixing notional with real satellites, it is best to choose an epoch

close to the real systems of interest.

The inclination, right ascension of the ascending node (RAAN), eccentricity, argument of perigee, and mean anomaly are all chosen according to the desired simulation. For example, a notional low Earth orbit constellation might consist of 225 satellites in 15 planes with 15 satellites per plane. The inclination might be chosen to be 90.0° to model a polar orbit. To provide somewhat even distribution of coverage around the equator, the RAAN of each plane could range from 0.0° to 168.0° in steps of 12.0° . Within the planes, the mean anomaly might likewise be spaced from 0.0° to 336.0° in steps of 24.0° .

3 Catalog-Derived Terms

Three of the remaining terms—the first and second derivative of the mean motion, and the drag term—can be derived from existing TLEs which are accessible in open repositories on the internet. We use a collection of 18,477 published TLEs associated with satellites, rocket bodies, and other debris. In order to assign terms to notional TLEs that represent realistic TLEs, the TLEs are categorized into low-Earth orbit (LEO), medium Earth orbit (MEO), geosynchronous (GEO), and highly elliptical orbit (HEO) populations.

The algorithm to assign TLEs to a population is given in Algorithm 1 and the impact of the included criteria is illustrated in Figure 1. There are various other criteria and algorithms, and the methods in this paper could be easily adapted by modifying Algorithm 1, including additional population categories.

With populations assigned, a mean value can be computed for the first and second derivative of the mean motion, and the drag term as shown in Table 1 and Figure 2.

4 Determining Mean Motion

A simple modification of Kepler’s third law allows the calculation of the mean motion in revolutions per day from the semi-major axis of orbit, as shown in

Population	$MM' \times 10^3$ (Rev/day ²)	$MM'' \times 10^6$ (Rev/day ³)	Drag Term $\times 10^3$ (R_{\oplus}^{-1})
HEO	0.048575 ± 0.384281	0.0125888 ± 0.120716	1.558450 ± 27.4125
LEO	0.154256 ± 3.778700	0.0942242 ± 2.866240	0.377655 ± 10.7492
MEO	0.154986 ± 1.640110	-0.0166109 ± 0.381907	1.295840 ± 48.6634
GEO	0.001190 ± 0.001467	0 ± 0	0.639138 ± 25.2697

Table 1: The mean and standard deviation values for the first and second derivative of the mean motion (MM' and MM'' , respectively), and the drag term, grouped by population.

Algorithm 1 TLE Classification

```

if Eccentricity  $\geq$  0.5 then
    HEO
else if Mean Motion  $\geq$  11.25 then
    LEO
else if Mean Motion  $\geq$  1.2 then
    MEO
else
    GEO

```

Equation 1:

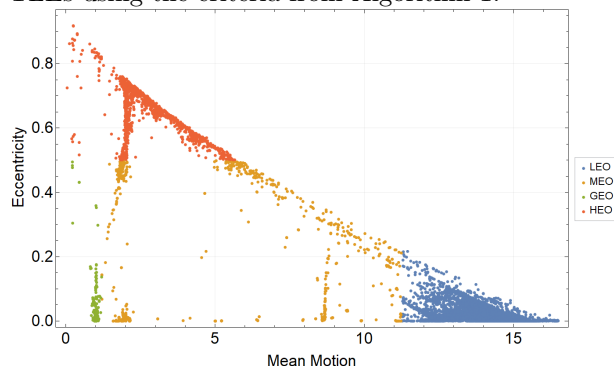
$$MM = \frac{T_{\oplus}}{2\pi} \sqrt{\frac{\mu}{a^3}} \quad (1)$$

where T_{\oplus} is a solar day (86,400 seconds), a is the semi-major axis, and μ is the standard gravitational parameter of Earth ($3.986004418 \times 10^{14} \text{m}^3/\text{s}^2$). The semi-major axis can be computed from the radius of the Earth R_{\oplus} , the altitude at perigee A_p , and the eccentricity e as shown in Equation 2.

$$a = \frac{A_p + R_{\oplus}}{1 - e} \quad (2)$$

The Earth’s radius R_{\oplus} is the distance from the center of the Earth to a point on its surface. Because the Earth is not a perfect sphere and due to the Earth’s topography, this radius is not constant across the Earth’s surface. The Earth can be modeled as an oblate spheroid with a minimum radius of 6,357 km at the poles, and a maximum radius of 6,378 km at the equator. For reference, analysis

Figure 1: The categorization of 18,477 published TLEs using the criteria from Algorithm 1.

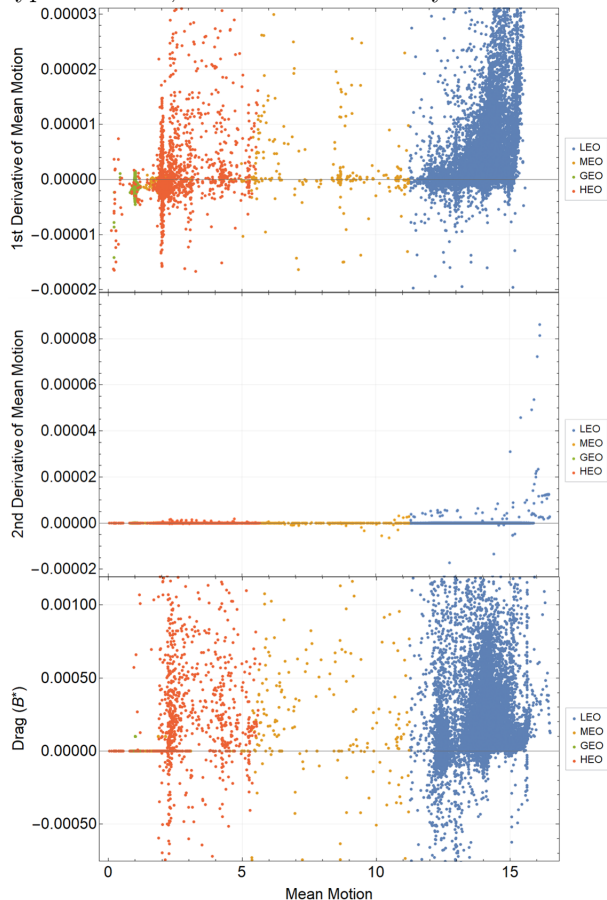


commonly relies on a nominal or “globally averaged” value of 6,371 km [8, 9]. Globally averaged values are computed by either

- Taking the mean of three radii measurements, two from the equator and one from a pole;
- Using the radius of a sphere with the same surface area as the Earth’s (authalic radius); or
- Using the radius of a sphere that has the same volume as the Earth spheroid (volumetric radius).

While it is possible to simply use a single value for the radius of the Earth such as a globally averaged value, this will present error in almost any simulation as will be quantified below. Instead, the value used for R_{\oplus} in Equation 2 should be relevant to the mean gravitational force that the satellite experiences as

Figure 2: The first and second derivative of the mean motion, and the drag term, highlighted by population type for all 18,477 TLEs in this study.



it travels around the non-spherical Earth. In other words, the value for R_{\oplus} should be the mean of the distance between the center of the Earth ellipsoid and the surface of the Earth directly under a satellite as it travels in its orbit. This study will refer to that value as the mean radius under the satellite, or R_s . Utilizing accurate numbers for this measure is imperative to generating realistic MMs, and consequently realistic TLEs. The following sections detail an approach to determine R_s and provides values that can be used in future simulations.

5 Mean Radius

This analysis assumes that the Earth is modeled as a WGS-84 ellipsoid[10]. The Earth ellipsoid also has variation in its gravitational potential as defined in the Earth Gravitational Model 2008[11] but this study focuses on SGP4 models that include the J2, J3, and J4 zonal harmonics coefficients. This study relies on the use of the Satrec package for python[12]. Satrec uses a satellite's TLE to compute the satellite's position and velocity for a given date and time.

To determine R_s , a satellite is propagated around the Earth and the geodetic latitude directly under the satellite is determined for many equally-spaced time steps throughout a simulation. Given each latitude, the radius of the ellipsoid at that position is calculated and stored in an array. Finally, the mean of these measurements over a simulation yields R_s . In the following sections, we describe a method for determining latitude directly from SGP4 propagation, and then our results for computing R_s from a large set of input inclinations, eccentricities, and arguments of perigee.

5.1 Determining Radii from Propagation

Given Cartesian coordinates for a satellite, we can convert them into latitude (ϕ), longitude (λ), and height (h). SGP4 propagation provides the ECEF coordinates for a satellite at all desired time steps in the simulation. The longitude is easily computed from the Cartesian coordinates as

$$\lambda = \text{ArcTan2}(y, x) \quad (3)$$

where ArcTan2 is the function that returns the angle from the origin, knowing which quadrant the position (x, y) lies in. The latitude and height can be computed by application of Ferrari's solution[13] which is not covered here.

For a given latitude ϕ , the radius of the ellipsoid at that latitude R_{ϕ} is given by

$$R_{\phi} = \sqrt{\frac{(R_e^2 \cos(\phi))^2 + (R_p^2 \sin(\phi))^2}{(R_e \cos(\phi))^2 + (R_p \sin(\phi))^2}} \quad (4)$$

For every time step in the simulation, we determine ϕ and therefore a value for R_ϕ . We then take the mean of all values for R_ϕ to determine R_s .

5.2 Results for R_s

The results in this paper are presented for orbits with inclinations varying from 0 to 90°, eccentricities ranging from 0 to 0.999, and arguments of perigee ranging from 0 to 90°. The choice of the altitude at perigee does not affect the results as long it creates a stable orbit. This analysis considered an altitude at perigee of 605.736 km for all runs.

For each choice of inclination, eccentricity, and argument of perigee, we determine R_s from a single orbit that is propagated with 1,000 equally spaced time steps. The number of orbits and steps per orbit can be increased but do not have a significant effect on the results. Furthermore, significantly increasing the number of orbits can introduce unwanted error due to the potentially degraded orbit modeled in SGP4 propagation.

The results provide a variation in R_s from 6358.669 km to 6378.137 km, partly illustrated in Figure 3. When computing MM, using R_s presents up to a $\sim 1.5\%$ correction as compared to using the typical WGS-84 mean radius of 6,371 km. To measure the impact of such a correction, TLEs are created using both the WGS-84 mean radius of the Earth and R_s . This results in two TLEs that are identical except for the MM. We repeat this process for the same ranges of inclinations, eccentricities, and arguments of perigee. The time for each pair of TLEs to drift 100 km apart is measured and illustrated in Figure 4.

In many cases, this drift can be greater than 100 km in less than only a few minutes. For many analyses such as conjunction analysis, object tracking, and coverage metrics, this accumulated error can present significant changes to the simulation results, especially for longer duration simulations. The method described above for determining R_s presents an improved means of positioning and modeling satellites through longer simulations.

Figure 3: Top: The mean radius of the Earth, under a satellite, as it propagates throughout its orbit. The red contour represents the commonly used mean radius of the Earth of 6,371.009 km. Bottom: The total percent error between a standard WGS-84 mean Earth radius of 6371.009 km and the method described in Section 5. The red contour represents where the difference is exactly zero. These contour plots were created with an argument of perigee of 0°.

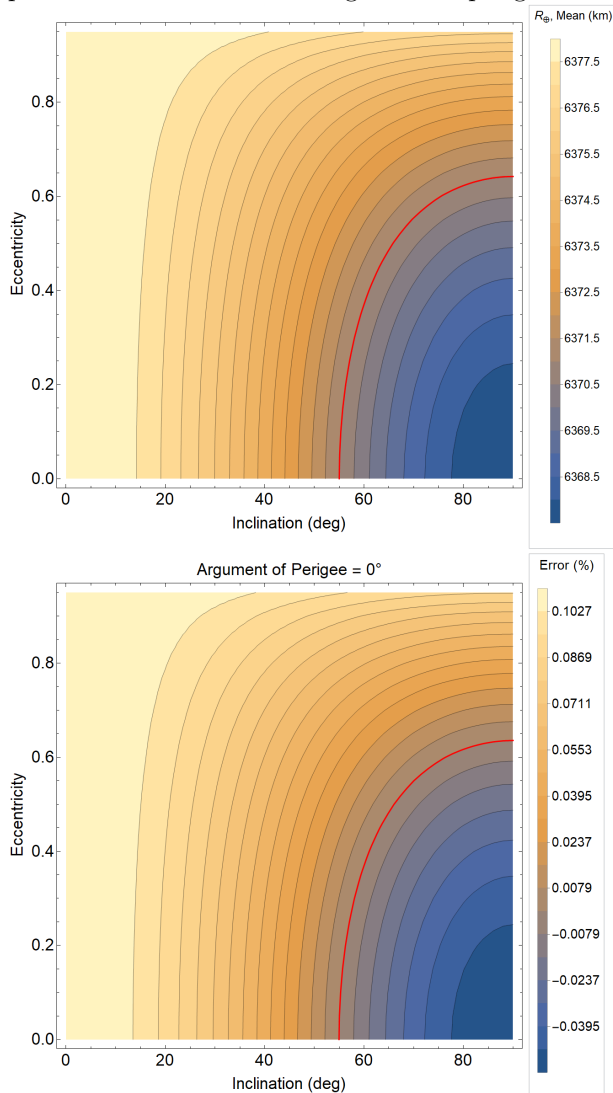
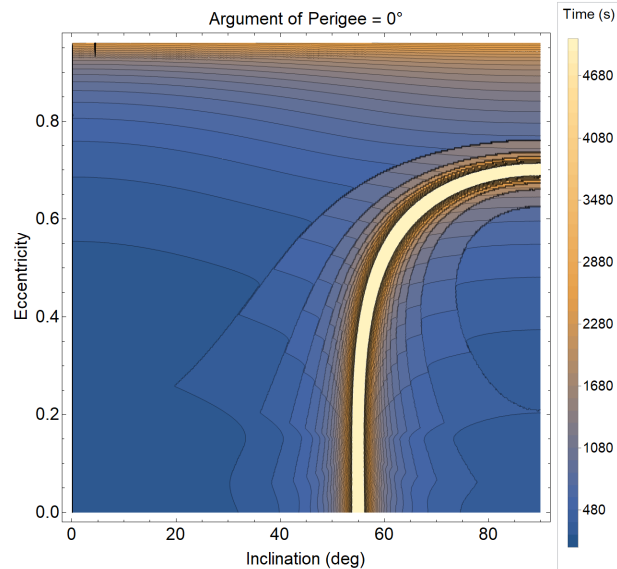


Figure 4: The time for two TLEs to drift 100 km, each with different assumptions for the Earth radius: one with a standard WGS-84 mean Earth radius, and one with an R_s value computed from Section 5. This contour plot was created with an argument of perigee of 0° .



6 Assembling Terms for Notional TLEs

With the catalog-derived terms ready, realistic TLEs can be created based on the desired inclination, eccentricity, argument of perigee, RAAN, and altitude at perigee. Table 2 lists all TLE terms, and whether they are derived from a catalog, determined by calculation, or taken as direct inputs.

The procedure for creating a TLE is as follows:

1. The desired inclination, eccentricity, altitude at perigee, and argument of perigee are chosen according to the desired orbit
2. The R_s value is determined based inclination, eccentricity, and argument of perigee
3. The semi-major axis is determined from Equation 2, substituting R_s in place of R_\oplus

Term	Method
First Derivative of MM	Catalog
Second Derivative of MM	Catalog
Drag (B^*)	Catalog
Inclination	Free
RAAN	Free
Eccentricity	Free
Argument of Perigee	Free
Mean Anomaly	Free
Mean Motion	Determined from R_s

Table 2: The TLE terms used in this study, and whether they are catalog-derived, free variables, or determined from other elements including the calculation of R_s as described in Section 5. All other TLE terms are trivially chosen except for the checksum which is computed based on all other entries in each line.

4. The MM is calculated from Equation 1
5. The satellite population is classified according to Algorithm 1 using the calculated MM and intended eccentricity
6. The first and second derivative of mean motion and drag terms are assigned from Table 1
7. The rest of the TLE elements are freely chosen, and the checksum is computed for the last character in each line

The simulated data for R_s described in Section 5 can be fit by a polynomial function whose parameters can be numerically determined. We fit a fifth-order 3-dimensional polynomial to the data for R_s with 56 parameters and determined a maximum difference of $5.47 \times 10^{-3} \%$ compared to directly simulating the orbit. This is across all inclinations, eccentricities, and arguments of perigee. Similarly, for an eighth-order polynomial with 165 parameters, the maximum difference was $0.93 \times 10^{-3} \%$ compared to direct simulation, across all values. The values for the parameters of the fifth-order polynomial are shown in Table 3. The polynomial with associated parameters is shown in Equation 5 with i , e , and ω the inclination, eccen-

tricity, and argument of perigee, respectively.

$$\begin{aligned}
R_s(i, e, \omega) = & c_{000} + c_{001}\omega + c_{002}\omega^2 + c_{003}\omega^3 + c_{004}\omega^4 + \\
& c_{005}\omega^5 + c_{010}e + c_{011}\omega e + c_{012}\omega^2 e + c_{013}\omega^3 e + \\
& c_{014}\omega^4 e + c_{020}e^2 + c_{021}\omega e^2 + c_{022}\omega^2 e^2 + c_{023}\omega^3 e^2 + \\
& c_{030}e^3 + c_{031}\omega e^3 + c_{032}\omega^2 e^3 + c_{040}e^4 + c_{041}\omega e^4 + \\
& c_{050}e^5 + c_{100}i + c_{101}i\omega + c_{102}i\omega^2 + c_{103}i\omega^3 + \\
& c_{104}i\omega^4 + c_{110}ie + c_{111}i\omega e + c_{112}i\omega^2 e + c_{113}i\omega^3 e + \\
& c_{120}ie^2 + c_{121}ie^2\omega + c_{122}ie^2\omega^2 + c_{130}ie^3 + \\
& c_{131}ie^3\omega + c_{140}ie^4 + c_{200}i^2 + c_{201}i^2\omega + c_{202}i^2\omega^2 + \\
& c_{203}i^2\omega^3 + c_{210}i^2e + c_{211}i^2e\omega + c_{212}i^2e\omega^2 + \\
& c_{220}i^2e^2 + c_{221}i^2e^2\omega + c_{230}i^2e^3 + c_{300}i^3 + c_{301}i^3\omega + \\
& c_{302}i^3\omega^2 + c_{310}i^3e + c_{311}i^3e\omega + c_{320}i^3e^2 + c_{400}i^4 + \\
& c_{401}i^4\omega + c_{410}i^4e + c_{500}i^5
\end{aligned} \tag{5}$$

7 Conclusion

We present a new means of creating TLEs for nonlunar satellites with realistic terms for mean motion, its first and second derivatives, and the drag term. The only inputs required are the desired inclination, eccentricity, argument of perigee, and altitude at perigee. The produced TLEs can be used in simulation alone or alongside TLEs from real satellites, and will behave like real systems. This increases the overall simulation accuracy for performance evaluation, conjunction analysis, and more. The methods described can be expanded to other classification schemes for different sets of populations.

Future work will involve investigating the satellite catalog and possibly deriving correlations among populations that could reduce the standard deviations in Table 1, though this may mean significantly increasing the complexity of population categorization. This work could also be adapted to include the EGM2008 terms and also regenerated for different satellite classification schemes[11].

Term	Value	Term	Value
c_{000}	6.377788×10^6	c_{112}	-9.972427×10^{-2}
c_{001}	2.836106×10^1	c_{113}	7.383957×10^{-4}
c_{002}	-4.915346×10^{-1}	c_{120}	9.150674×10^1
c_{003}	-4.017214×10^{-3}	c_{121}	-1.33747×10^0
c_{004}	1.273759×10^{-4}	c_{122}	1.155062×10^{-3}
c_{005}	-5.643483×10^{-7}	c_{130}	4.645793×10^0
c_{010}	2.120874×10^3	c_{131}	-1.909859×10^0
c_{011}	-1.886565×10^2	c_{140}	5.290634×10^1
c_{012}	5.241726×10^0	c_{200}	-3.926748×10^0
c_{013}	-3.84173×10^{-2}	c_{201}	1.703196×10^{-2}
c_{014}	-2.268633×10^{-6}	c_{202}	-8.207037×10^{-6}
c_{020}	-3.447518×10^3	c_{203}	2.674298×10^{-8}
c_{021}	8.553227×10^1	c_{210}	4.368207×10^0
c_{022}	-4.719285×10^0	c_{211}	-9.744218×10^{-2}
c_{023}	3.438466×10^{-2}	c_{212}	-8.298287×10^{-6}
c_{030}	9.952275×10^3	c_{220}	2.116514×10^{-1}
c_{031}	1.634122×10^2	c_{221}	-4.547244×10^{-4}
c_{032}	5.259614×10^{-2}	c_{230}	-9.768337×10^{-2}
c_{040}	-1.695787×10^4	c_{300}	1.323687×10^{-3}
c_{041}	-8.008678×10^1	c_{301}	-1.327782×10^{-4}
c_{050}	8.501297×10^3	c_{302}	5.032226×10^{-8}
c_{100}	2.948006×10^1	c_{310}	-3.319618×10^{-2}
c_{101}	-1.151884×10^0	c_{311}	7.264131×10^{-4}
c_{102}	1.653916×10^{-2}	c_{320}	-5.846808×10^{-4}
c_{103}	-1.276845×10^{-4}	c_{400}	4.655915×10^{-4}
c_{104}	3.521573×10^{-8}	c_{401}	6.438237×10^{-8}
c_{110}	-1.676297×10^2	c_{410}	4.999741×10^{-6}
c_{111}	6.645437×10^0	c_{500}	-2.08623×10^{-6}

Table 3: The parameters for a fifth-order polynomial fit of the R_s data across all inclinations, eccentricities, and arguments of perigee from Section 5.

Acknowledgments

This technical data was produced for the U. S. Government under Contract No. FA8702-22-C-0001, and is subject to the Rights in Technical Data-Noncommercial Items Clause DFARS 252.227-7013 (FEB 2014). © 2022 The MITRE Corporation. All Rights Reserved. DISTRIBUTION A: Approved for public release; distribution unlimited. Public Release Case Number 22-0304.

References

- [1] Ucs satellite database, May 2021. URL <https://www.ucsusa.org/resources/satellite-database>. <https://www.ucsusa.org/resources/satellite-database>.
- [2] Jason A. Parish. Optimizing coverage and revisit time in sparse military satellite constellations; a comparison of traditional approaches and genetic algorithms, 2004. URL <https://calhoun.nps.edu/handle/10945/1209>.
- [3] Nozomi Hitomi and Daniel Selva. Constellation optimization using an evolutionary algorithm with a variable-length chromosome. In *2018 IEEE Aerospace Conference*, pages 1–12, 2018. doi: 10.1109/AERO.2018.8396743.
- [4] Irene A. Budianto and John R. Olds. Design and deployment of a satellite constellation using collaborative optimization. *Journal of Spacecraft and Rockets*, 41(6):956–963, 2004. doi: 10.2514/1.14254. URL <https://doi.org/10.2514/1.14254>.
- [5] David Vallado, Paul Crawford, Richard Hujzak, and T.S. Kelso. Revisiting spacetrack report #3. *AIAA/AAS Astrodynamics Specialist Conference and Exhibit*, 2012. doi: 10.2514/6.2006-6753. URL <https://arc.aiaa.org/doi/abs/10.2514/6.2006-6753>.
- [6] T S Kelso. Norad two-line element set format, Dec 2019. URL <https://www.celestrak.com/NORAD/documentation/tle-fmt.php>. <https://www.celestrak.com/NORAD/documentation/tle-fmt.php>.
- [7] David Vallado and Paul Cefola. Two-line element sets - practice and use. *Proceedings of the International Astronautical Congress, IAC*, 7:5812–5825, 01 2012.
- [8] EE Mamajek, A Prsa, G Torres, P Harmanec, M Asplund, PD Bennett, N Capitaine, J Christensen-Dalsgaard, E Depagne, WM Folkner, et al. Iau 2015 resolution b3 on recommended nominal conversion constants for selected solar and planetary properties, arxiv151007674 astro-ph, 2015.
- [9] Helmut Moritz. Geodetic reference system 1980. *Bulletin géodésique*, 54(3):395–405, 1980.
- [10] W.D. McClain and D.A. Vallado. *Fundamentals of Astrodynamics and Applications*. Space Technology Library. Springer Netherlands, 2001. ISBN 9780792369035. URL <https://books.google.com/books?id=PJL1WzMBKjkC>.
- [11] Nikolaos K. Pavlis, Simon A. Holmes, Steve C. Kenyon, and John K. Factor. The development and evaluation of the earth gravitational model 2008 (egm2008). *Journal of Geophysical Research: Solid Earth*, 117(B4), 2012. doi: <https://doi.org/10.1029/2011JB008916>. URL <https://agupubs.onlinelibrary.wiley.com/doi/abs/10.1029/2011JB008916>.
- [12] Brandon Rhodes. python-sgp4. <https://github.com/brandon-rhodes/python-sgp4>, 2021.
- [13] J. Zhu. Conversion of earth-centered earth-fixed coordinates to geodetic coordinates. *IEEE Transactions on Aerospace and Electronic Systems*, 30(3):957–961, 1994. doi: 10.1109/7.303772.